Hindawi
International Journal of Corrosion
Volume 2018, Article ID 4121506, 8 pages
https://doi.org/10.1155/2018/4121506

Research Article

Characterization of Sludge Deposits from Refineries and Gas Plants: Prerequisite Results Requirements to Facilitate Chemical Cleaning of the Particular Equipment

Rasha A. Al-Ghamdi and Husin Sitepu

Research & Development Center, Saudi Aramco, P.O. Box 62, Dhahran, Saudi Arabia

Correspondence should be addressed to Rasha A. Al-Ghamdi; rasha.ghamdi@aramco.com

Received 6 February 2018; Accepted 24 May 2018; Published 2 September 2018

Academic Editor: Flavio Deflorian

In this paper, the method developed by the authors to separate the inorganic materials from the hydrocarbon of the sludge deposits, which is fast and can accurately identify very small quantities of inorganic materials, has been extended to characterize the 12 types of sludge samples collected from (a) a regeneration overhead acid gas condenser, (b) water draw-off pump's suction strainer in a gas plant, and (c) condenser, inside vessels of inlet head, and head coiler tube equipment at gas plants. The results revealed that the major phases are (a) iron sulfide corrosion products with the hydrocarbon type of mixture of diesel and lube oil for a condenser and (b) carbonate scale in the form of calcium carbonate with the hydrocarbon type of lubricant oil for sludge deposits from a suction strainer for pumps, and drilling mud in the form of barium sulfate with no organic hydrocarbon or polymer for sludge samples from a water recycling pump. Moreover, the major phases for inorganic materials built up in a condenser, inside the vessel's inlet head, and the head coiler tube revealed that iron oxide corrosion products are found in the steam drum, and iron sulfate corrosion products are built up in the condenser. The presence of dissolved oxygen in the boiler feed water is indicated by a high wt% of iron oxide corrosion product in the form of magnetite (Fe_3O_4), which appeared in the inorganic materials built up in the condenser steam drum. Knowing accurately which phases and their wt% were involved in the inorganic materials can guide the field engineers to facilitate efficient cleaning of the equipment by drawing up the right procedures and taking preventive action to stop the generation of those particular sludge deposits.

1. Introduction

The sludge deposits that frequently accumulate inside the equipment used in the oil industry can cause failures and temporarily shut down the refinery and gas plants [1]. Sitepu, Al-Ghamdi, and Zaidi (2017) successfully experimented to separate the inorganic materials (i.e., the insoluble part or non-hydrocarbon) from the hydrocarbon (dichloromethane soluble part) of the sludge deposits that were collected from the diesel oil tank in a refinery and accurately identified and quantified the very small quantity of inorganic materials, Figure 1. They showed that the X-ray powder diffraction (XRD) data consisted of iron oxide corrosion products in the form of goethite [FeO(OH)], magnetite [Fe_3O_4] and lepidocrocite [FeO(OH)], iron sulfide corrosion products in the form of pyrite [FeS_2] and pyrrhotite [Fe_7S_8], and formation materials in the form of quartz [SiO_2]. Additionally, Sitepu, Al-Ghamdi, and Zaidi (2017) [1] showed the relationship between their XRD phase identification results of the sludge samples that were generated in the particular equipment in refineries and gas plants, and the nature of the corrosion and scale products, Table 1.

Subsequently, Sitepu, Al-Ghamdi, and Zaidi (2017) [1] described that the gas chromatography mass spectrometry (GCMS) analysis results of the hydrocarbon (dichloromethane soluble part) showed diesel with the carbon range (C10 to C27), which suggests the minor portion of the oil-based type of sludge deposits was a diesel. Additionally, thermal gravimetric analysis (TGA) yielded that weight percentage (wt%) of inorganic compound, water, and hydrocarbon soluble were 3 wt%, 25 wt%, and 72 wt%, respectively. Knowing which phases and their wt% were involved in the inorganic

Table 1: Summary of the identified phases of the inorganic materials (i.e., the insoluble part or nonhydrocarbon) separated from the hydrocarbon (dichloromethane soluble part) of the sludge deposits, and its nature [1].

The Identified Phases	Nature of the Corrosion and Scale Products
Magnetite (Fe_3O_4) Lepidocrocite (FeOOH) Goethite (FeOOH) Akaganeite (FeOOH)	Iron Oxide Corrosion Product: (i) At a high temperature magnetite corrosion products it will coat the iron/steel to prevent oxygen to reach underlying metal. Mostly, at low temperature, lepidocrocite formed and with time it transformed into most stable goethite. Akaganeite formed in marine environments.
Gregite (Fe_3S_4) Pyrite (FeS_2) Marcasite (FeS_2) Mackinawite ($FeS_{0.9}$) Pyrrhotite (Fe_7S_8)	Iron Sulfide Corrosion Products: (i) Pyrophoric iron sulfide (pyrrhotite-FeS) results from the corrosive action of sulfur or sulfur compounds (H_2S) on the iron (steel) and moisture.
Iron Chloride ($FeCl_3$) Iron Chloride Hydrate ($FeCl_2$-$4H_2O$)	Chloride corrosion products
Calcite ($CaCO_3$) Aragonite ($CaCO_3$) Siderite ($FeCO_3$)	Carbonate scale
Basanite ($CaSO_4$. $2H_2O$) Anhydrite ($CaSO_4$) Gypsum ($CaSO_4$. $2H_2O$)	Sulfate scale
Quartz (SiO_2) Albite ($NaAlSi_3O_8$) Microcline ($KAlSi_3O_8$) Cristoballite (SiO_2)	Formation material: (i) Normally found in the sandstone or sand
Illite ($(K_5(AlFeMg)_3(SiAl)_4O_{10}(OH)_2$)	Clay minerals normally found with sandstone
Ettringite ($Ca_6Al_2(SO_4)_3(OH)_{12}$)	Cementing material
Barite ($BaSO_4$)	Drilling mud
Aluminum Oxide (Al_2O_3)	Normally from catalyst
Sulfur (S)	
Sodium Iron Oxide ($NaFeO_2$)	

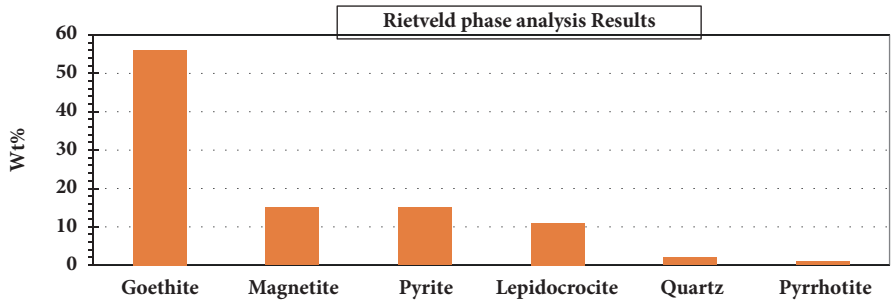

Figure 1: Rietveld phase analysis results of inorganic materials (insoluble part) [1].

materials [2] along with the type of hydrocarbon that presents at the sludge deposits can guide the engineers at the affected refinery and gas plants to overcome the problems by devising appropriate corrective procedures.

The main objective of the present study was to extend the new method developed by Sitepu, Al-Ghamdi, and Zaidi (2007) [1] to particularly and accurately examine the phase composition of inorganic materials (non-soluble or non-hydrocarbon) that were built up in the different equipment at refineries and gas plants — (a) a regeneration overhead acid gas condenser located at the low-pressure gas treating unit, (b) water draw-off pumps suction strainer for pumps and water recycle pump in a gas plant, and (c) condenser, inside vessels of inlet head, and head coiler tube of the sulfur recovery unit (SRU) — using advanced XRD [3–9] and Rietveld method [10–18], which are well-known techniques, both for identification of phases and for the quantification [19–24] of all the identified phases. Subsequently, when the types of

Table 2: The description of the sludge samples investigated in this study.

Sample	Sludge Deposits Collected from	Use of Sitepu and Zaidi (2017) [1] Method of Sample Preparation Procedures	Why the Phase Compositions are Required?
XRPD-A	Regeneration overhead acid gas condenser located at the low-pressure gas treating unit.	The deposits were treated with dichloromethane, and then filtered in the filtration assembly. The (i) insoluble part (i.e., inorganic materials or non-hydrocarbon) was analyzed by advanced XRD and Rietveld method; (ii) hydrocarbons (dichloromethane soluble part) was analyzed by GCMS.	The results assist the field engineers to identify the cause of the accumulated sludge deposits and provide corrective remedies.
XRPD-B XRPD-C	Water draw off pump's suction strainer in a gas plant suction strainer for pumps, to determine the water recycle pump.		Knowing which phases were involved in the deposits can guide the field engineers and source of materials found XRPD-C in the suction strainer, and identify the root cause of the repetitive pumps trips.
XRPD-D	Condenser tube side #1	Sulfur type of deposits were directly analyzed by the advanced XRD and Rietveld method without any pre-treatment.	Thick deposits of various types of mineral scales accumulated in the SRU process equipment can cause one of the major operational problems. The phase composition results can guide the engineers to overcome the problems by devising the right corrective procedures.
XRPD-E	Condenser #4		
XRPD-F	Condenser manway cover		
XRPD-G	Inside vessel of inlet head		
XRPD-H	Heat coiler tube		
XRPD-I	Condenser #1 tubes		
XRPD-J	Condenser #1 inlet head		
XRPD-K	Condenser #4 tubes		
XRPD-L	Condenser steam drum		

the hydrocarbon were required by the field engineers for the particular deposits, the authors independently analyzed the dichloromethane soluble part.

2. Experimental Procedure

In the present study, the limitation of the new method of sample preparation procedures developed by Sitepu, Al-Ghamdi, and Zaidi (2017) [1] has been extended and to characterize the inorganic materials present in the as-received sludge deposits from many different parts and locations of equipment in Saudi Aramco's refineries and gas plants. Table 2 shows the description of the samples investigated in this study.

The accurate phase identification and quantification results of inorganic materials or the insoluble part, Table 2, are a prerequisite, which is required to facilitate chemical cleaning [2] of the particular failure equipment and prevent the reoccurrence. Therefore, the inorganic materials were manually ground by an agate mortar and a pestle for several minutes to achieve a fine particle size [18]. Then, the fine powders were mounted into the sample holders by front pressing. Furthermore, high-resolution XRD data of the samples were measured using the Rigaku ULTIMA-IV X-ray powder diffractometer with a copper X-ray tube from 4° to 75° 2θ Bragg-angles with a step size of 0.04° and counting time of 1° per minute.

Subsequently, all of the XRD data sets of the inorganic materials — (Table 2) — were then identified by High Score Plus software [15] (X'Pert High Score Plus Version 3.0e PANalytical Inc.) combined with the International Powder Diffraction Data (ICDD) of the powder diffraction file (PDF-4+) database of the standard reference materials. When all the phases are identified accurately, the authors subsequently use the Rietveld method [10–18], which adjusts the refinable parameters until the best fit of the entire calculated pattern to the entire measured XRD pattern is achieved, to determine the quantitative phase analysis [19–24] or wt%, W_p, for each of these identified phases, p, is proportional to the product of the scale factor, s, as derived in the Rietveld phase analysis, with the mass and volume of the unit cell and is given by

$$W_p = \frac{S_p\,(ZMV)_p}{\sum_{i=1}^{n} S_i\,(ZMV)_i} \quad (1)$$

where Z, M, and V are the number of formula units per unit cell, the mass of the formula unit, and the unit-cell volume (in Å^3), respectively. The advantages of the Rietveld method [10–18] are as follows:

(i) The calibration constants are computed from simple literature data (i.e., Z, M, and V values) rather than by laborious experimentation.

(ii) All reflections in the pattern are explicitly included, irrespective of overlap.

(iii) The background is better defined since a continuous function is fitted to the whole powder diffraction pattern.

(iv) The preferred orientation effects [18] can be corrected and determined.

(v) The crystal structural and peak-profile parameter scan can be refined as part of the same analysis.

2.1. Reproducibility. Scarlett et al. (2002) [25] described that one of the main sources of error to perform accurately quantitative phase analysis of high quality of high-resolution XRD data by Rietveld method is microabsorption, which is the presence of absorption contrast between phases. In some circumstances, they showed that the microabsorption proves to be challenging. In this paper, the limited amount of inorganics deposits (i.e., non-hydrocarbon parts) was manually ground in an agate mortar and a pestle for several minutes to

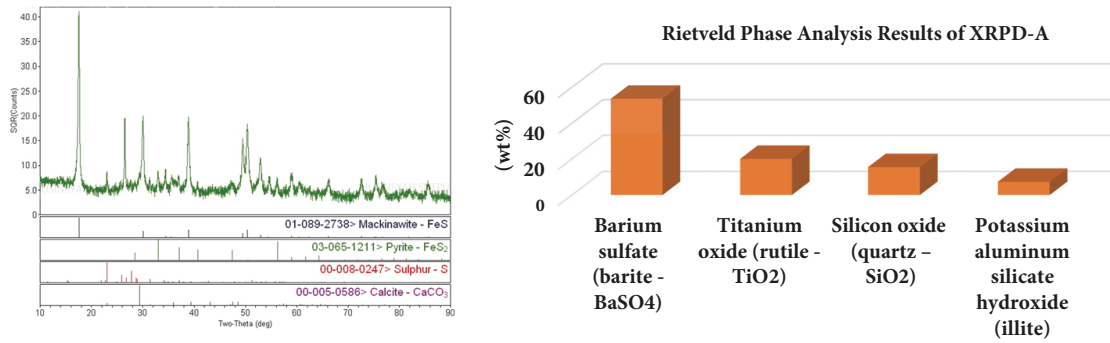

(a) XRD phase identification results (b) Rietveld phase analysis results

Figure 2: (a) XRD phase identification results of the inorganic deposits present in the sludge deposits (XRPD-A) along with the identified mineral reference patterns. (b) The wt% of the identified phases obtained from the Rietveld method.

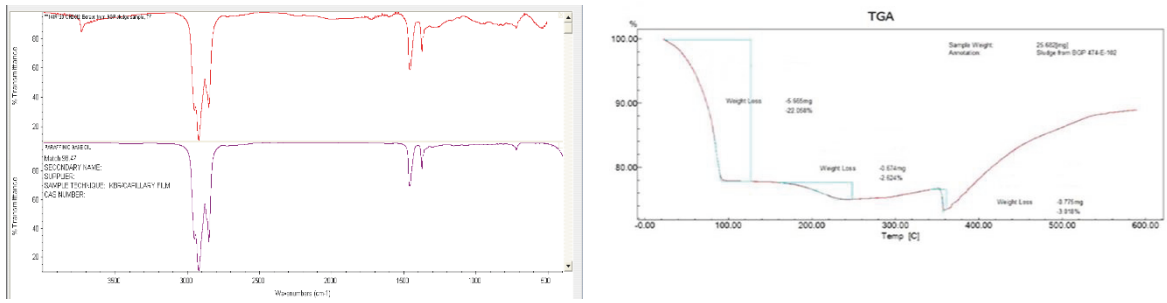

(a) FTIR (b) TGA

Figure 3: (a) The FTIR spectra confirmed that the hydrocarbon (dichloromethane soluble part) mainly contained hydrocarbon. (b) The TGA spectra showed that the sample lost around: (a) 22% of its original weight at 100°C, which represents moisture and volatile hydrocarbons; and (b) 2.6% of its weight from 100°C to 250°C representing heavy hydrocarbons.

achieve fine particle size [18] and eliminate microabsorption effects. To reproduce the results, the sample preparations were carefully repeated—the size distribution of the limited amount of inorganic deposits was modified by McCrone micronizing mill in order to achieve inadequate intensity reproducibility [26]. Excellent agreement was obtained between the results of the two experiments (i.e., McCrone mill-micronizing and manually ground in an agate mortar and a pestle techniques); and following O'Connor et al. [26] — the microabsorption correction was not conducted — in the refinement. The results of the manually ground in an agate mortar and a pestle for several minutes are quoted here as the experimental data of the limited amount of inorganics deposits (i.e., non-hydrocarbon parts) were superior quality in terms of counting statistics.

3. Results and Discussions

3.1. Regeneration Overhead Acid Gas Condenser Located (XRPD-A). The XRD phase identification result of the inorganic materials (insoluble part or non-hydrocarbon) revealed that the deposits consisted of corrosion products in the forms of iron sulfide (e.g., mackinawite-FeS and FeS_2) with some additional amounts of brimstone (sulfur), carbonate scale in the form of calcium carbonate with the mineral name of calcite ($CaCO_3$), Figure 2(a). When Rietveld refinement was conducted to determine the phase composition for each of the identified phases, the results revealed 92.8 wt% of iron sulfide corrosion product (e.g., 89.9 wt% of mackinawite-FeS and 2.9 wt% of FeS_2) with the addition of 6.0 wt% of sulfur (S), and 2.1 wt% of calcium carbonate [calcite ($CaCO_3$)], Figure 2(b).

The GCMS analysis of hydrocarbon (dichloromethane soluble part) revealed that the sample looks waxy extending to > C35; however, it looks like the sample contains two different hydrocarbon-based products as suggested by the bimodal profile of the selected ion chromatogram. The light end part of this bimodal is diesel range hydrocarbons, whereas the heavy end of the profile is suggested to be lube/seal oil of some sort as it is supported by the fact that an antioxidant has been identified in the sample. The antioxidant is usually a diagnostic of lube/seal oil in this case. To confirm the results, the Fourier transformed infrared (FTIR) and thermal gravimetric analysis (TGA) analyses were required.

The Fourier-transform infrared spectroscopy (FTIR) results confirmed that the extracted sample from the sludge contained mainly hydrocarbon, Figure 3(a). The TGA results showed that the sample lost around 22% of its original weight at 100°C, which represents moisture and volatile hydrocarbons. Also, the sample lost 2.6% of its weight from 100°C to 250°C representing heavy hydrocarbons, Figure 3(b). The

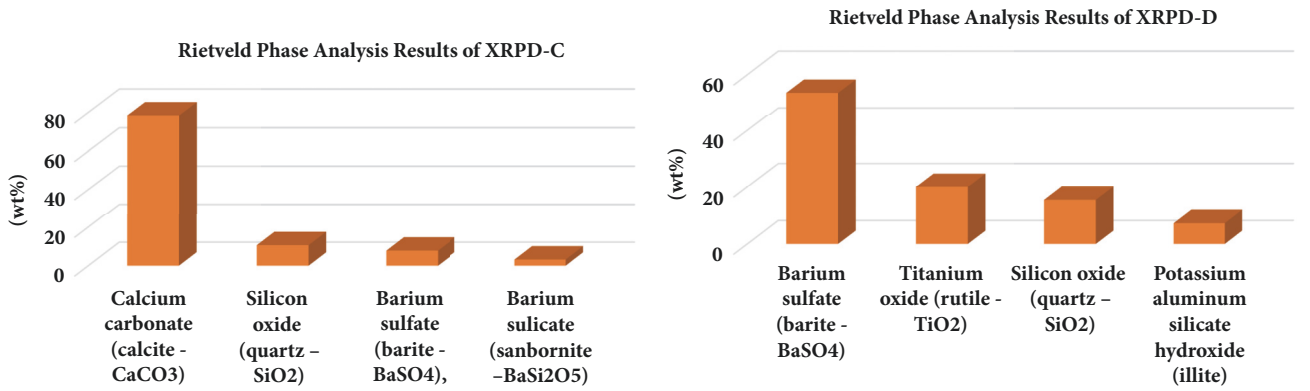

(a) XRPD-B (b) XRPD-C

Figure 4: The Rietveld phase analysis results (i.e., wt% of the identified phases) of inorganic deposits (insoluble or nonhydrocarbon part) present in the (a) suction strainer for pumps (XRPD-B) and (b) water recycle pump (XRPD-C).

FTIR and TGA results demonstrated that the sample contains paraffinic-based hydrocarbons (25.0 wt%), which is most probably a mixture of diesel and lube oil. The lube oil content is also confirmed by the presence of the antioxidant. The diesel is used as a carrier of different oil field chemicals, such as corrosion inhibitors.

It can be summarized that the new method developed by Sitepu, Al-Ghamdi, and Zaidi (2017) [1] worked well in this study to characterize the inorganic deposits (insoluble part) buildup in regeneration overhead acid gas condenser located (XRPD-A). The advanced XRD and Rietveld method results revealed the inorganic deposits mainly consists of corrosion products in the form of iron sulfide. Additionally, the hydrocarbon (dichloromethane soluble part) revealed that the sample contains paraffinic-based hydrocarbons (25.0 wt%) suggesting that it is the mixture of diesel and lube oil. The presence of the antioxidant confirmed the lube oil; and the diesel is usually used as a carrier of different oil field chemicals such as corrosion inhibitors. The findings helped the investigation team to identify the root source of the sludge accumulation and provide the corrective remedies.

3.2. Water Draw-Off Pump's Suction Strainer in a Gas Plant — Suction Strainer for Pumps (XRPD-B) and Water Recycle Pump (XRPD-C). The results revealed that the inorganic deposits part from suction strainer for pumps (XRPD-B) consisted of carbonate scale in the form of calcium carbonate with the mineral name of calcite ($CaCO_3$), formation sandstones in the form of silicon oxide with the mineral name quartz (SiO_2), drilling muds in the form of barium sulfate with the mineral name of barite ($BaSO_4$), and barium silicate (sanbornite ($BaSi_2O_5$)). Additionally, the inorganic deposit part from the water recycle pump (XRPD-B) consisted of barium sulfate (barite ($BaSO_4$)), titanium oxide (rutile (TiO_2)), silicon oxide (quartz (SiO_2)), potassium aluminum silicate hydroxide (illite), calcium carbonate (calcite ($CaCO_3$)), and aluminum zinc (of $Al_{0.71}Zn_{0.91}$). The X-ray fluorescence (XRF) findings support the XRD results. The phase composition — wt% for each of the identified phases — results obtained from the Rietveld method revealed that the inorganic part (i.e., non-hydrocarbon) present in the sludge from the suction strainer for pumps (XRPD-B) consisted of 78.4 wt% of calcium carbonate in the form of $CaCO_3$, 10.6 wt% of formation sandstone or sand in the form of SiO_2, 7.8 wt% of drilling mud in the form of $BaSO_4$, and 3.1 wt% of barium silicate (sanbornite ($BaSi_2O_5$)), Figure 4(a).

Moreover, the phase composition (wt% for each of the identified phases) results obtained from the Rietveld method revealed that the inorganic part (i.e., non-hydrocarbon) present in the sludge from the water recycle pump (XRPD-C) consisted of 53.6 wt% of $BaSO_4$, 20.0 wt% of TiO_2, 15.4 wt% of SiO_2, 7.3 wt% of illite, 3.4 wt% of $CaCO_3$, and 0.1 wt% of $Al_{0.71}Zn_{0.91}$, Figure 4(b). The XRF findings support the XRD results. The results obtained from the XRD chemical identification and composition of the identified phases helped the engineers at the affected refinery and gas plants to determine the source of the materials found in the suction strainer and overcome the problems by devising appropriate corrective procedures.

The composition analysis of the hydrocarbon (dichloromethane soluble part) presents the sludge samples from the suction strainer (XRPD-B) and water recycle pump (XRPD-C) obtained from FTIR, DSC, and TGA indicated that the (a) sample is mostly organic and its phenolic-based material, (b) glass transition temperature (Tg) of the sheet sample material was 102°C (I), (c) total weight loss of volatiles (organic-based volatiles/light components) and organic-based materials were determined to be about 76 wt%, and (d) the remaining residual mass of the sample (inorganic) was found to be around 24 wt%. The FTIR compositional analysis results show that the sample is similar to a bisphenol-based polymeric material. Additionally, the differential scanning calorimetry (DSC) result showed that the Tg of the sheet sample material was 1°C. Moreover, the TGA results showed that the percentage of the total losses of the sample was 76 wt%, and the residual mass was 24 wt%.

The GCMS analysis of the hydrocarbon (dichloromethane soluble part) from the suction strainer for pumps (XRPD-B) revealed high boiling hydrocarbon components from C13 to C30+, which could indicate either heavy petroleum

material or a certain type of lubricant oil. The Fourier Transform Ion Cyclotron Resonance Mass Spectrometry (FT-MS) analysis further indicated the presence of a polymeric material that was identified as nylon 7 oligomers with four to 13 repeat units. Nylon 7, also referred to as polyamide 7, may generally be used in fiber materials, films, or thermoplastic parts, but inclusion in oil field chemical formulations might also be possible, so that the ultimate source remains unknown. Note that the sludge samples collected from the suction strainer for sludge samples collected from the water recycle pump (XRPD-C) did not contain a significant trace of hydrocarbon and polymeric components as evidenced by the GCMS and FT-MS analyses, indicating that the sample contains either no, or much less, organic hydrocarbons or polymers.

Based on the XRD results, it can be highlighted that the inorganic part (i.e., nonhydrocarbon) present at the sludge deposits from (a) the suction strainer for pumps (XRPD-B) mainly consisted of $CaCO_3$ with the type of high boiling hydrocarbon components from C13 to C30+ suggesting that either heavy petroleum material or a certain type of lubricant oil hydrocarbon and (b) the water recycle pump (XRPD-C) mainly consisted of $BaSO_4$ and it does not have either organic hydrocarbons or polymers. The XRF findings support the XRD results and can help the engineers at the affected gas plant to identify the root causes of the sludge deposits and develop remedial action plan to avoid reoccurrence.

3.3. Deposits from Condenser, Inside Vessels of Inlet Head, and Head Coiler Tube of the Sulfur Recovery Unit (SRU). Figure 5(a) shows the quantitative phase analysis results of the identified phases obtained from the Rietveld method for the inorganic deposits buildup in (a) condenser tube side #1 (XRPD-D), (b) condenser #4 (XRPD-E), and (c) condenser manway cover (XRPD-F). The results showed that the XRD data of the deposits mainly consist of an iron sulfate corrosion product, along with some sodium and ammonium iron sulfate corrosion products. For deposits that were collected from condenser tube side #1 (XRPD-D) and condenser manway cover (XRPD-F), the highest Rietveld phase analysis of the identified phases (wt%) is an iron sulfate corrosion product. For deposits collected from condenser #4 (XRPD-E), ammonium sulfate is the highest quantitative phase analysis of the identified phases (wt%) obtained from the Rietveld method. Additionally, sodium iron sulfate appears as the minor phase in condenser tube side #1 (XRPD-D) and condenser tube side #1 (XRPD-D), but not in the condenser manway cover (XRPD-F). While iron sulfite is not detected in either condenser tube side #1 (XRPD-D) or condenser manway cover (XRPD-F), it appears in condenser #4 (XRPD-E). Iron sulfate hydroxide is the trace material found in condenser tube side #1 (XRPD-D), and ammonium iron sulfate hydroxide is the trace material found in the condenser manway cover (XRPD-F).

Figure 5(b) depicts the Rietveld phase analysis results of the inorganic deposits buildup in (a) the inside vessel of the inlet head (XRPD-G), (b) the head coiler tube (XRPD-H), (c) the condenser #1 tubes (XRPD-I), (d) the condenser #1 inlet head (XRPD-J), (e) the condenser #4 tubes (XRPD-K), and (f) the condenser steam drum (XRPD-L). The results revealed that the Rietveld phase analysis—wt% for each of the identified phases—showed that the major phases are (a) iron sulfate corrosion product in the form of pyrrhotite (Fe_7S_8) both for the inorganic deposits built up inside the vessel of the inlet head (XRPD-G) and condenser #1 inlet head (XRPD-J), (b) ferrinatrite [$Na_3Fe(SO_4)_3.3H_2O$] both for the inorganic deposits built up in the head coiler tube (XRPD-H) and the condenser #1 tubes (XRPD-I), and (c) ammonium iron sulfate [$(NH_4)_2Fe_2(SO_4)_3$] for the inorganic deposits built up in #4 tubes (XRPD-K); and iron oxide corrosion products in the form of Fe_3O_4 and hematite (Fe_2O_3) for the inorganic deposits built up in the condenser steam drum (XRPD-L). The presence of dissolved oxygen in the boiler feed water is indicated by a high wt% of Fe_3O_4 phase appeared in the inorganic deposits built up in the condenser steam drum (XRPD-L).

It can be highlighted that the new method developed by Sitepu, Al-Ghamdi, and Zaidi (2017) [1] worked well in this study to characterize the inorganic deposits built up in the SRU [9] affected equipment such as (a) the condenser tube side #1 (XRPD-D), (b) the condenser #4 (XRPD-E), (c) the condenser manway cover (XRPD-F), (d) the inside vessel of the inlet head (XRPD-G), (e) the head coiler tube (XRPD-H), (f) the condenser #1 tubes (XRPD-I), (g) the condenser #1 inlet head (XRPD-J), (h) the condenser #4 tubes (XRPD-K), and (i) the condenser steam drum (XRPD-L). Knowing which phases quantitatively were involved in the inorganic material buildup in the SRU equipment can guide the engineers at the affected refinery and gas plants to facilitate efficient cleaning of the equipment by drawing up the right procedures and taking preventive action.

4. Conclusions

In this paper, the method developed by Sitepu, Al-Ghamdi, and Zaidi (2017) [1] has been extended to characterize the 12 types of the inorganic deposit built up in (a) a regeneration overhead acid gas condenser, (b) water draw-off pump's suction strainer in a gas plant, and (c) condenser, inside vessels of the inlet head, and head coiler tube of the sulfur recovery unit (SRU). Based on the advanced XRD and Rietveld method results it can be concluded that the inorganic deposits (soluble part) built up in the following:

(i) A regeneration overhead acid gas condenser mainly consists of a corrosion product in the form of iron sulfide, which might be caused by the corrosive action of sulfur or sulfur compounds (H_2S) on the iron (steel) and moisture. Additionally, the hydrocarbon (dichloromethane soluble part) contained paraffinic-based hydrocarbons, which suggests the mixture of diesel and lube oil.

(ii) A suction strainer for pumps mainly consisted of carbonate scale calcium carbonate in the form of calcite ($CaCO_3$) suggesting that it is due to the carbonate scale. Moreover, the type of hydrocarbon is either a heavy petroleum material or a certain type of lubricant oil hydrocarbon.

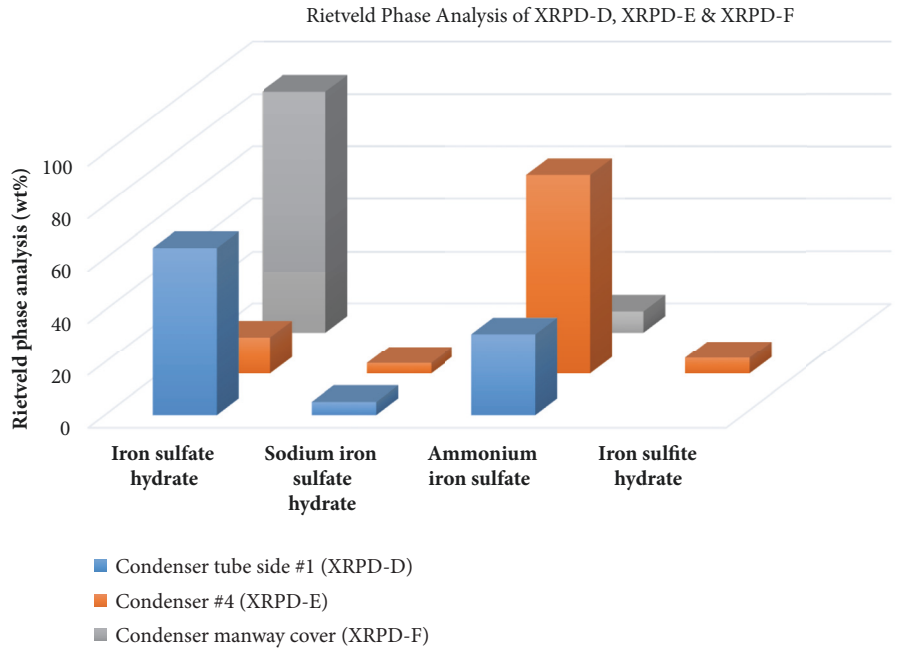

(a) Rietveld phase analysis of XRPD-D, XRPD-E and XRPD-F

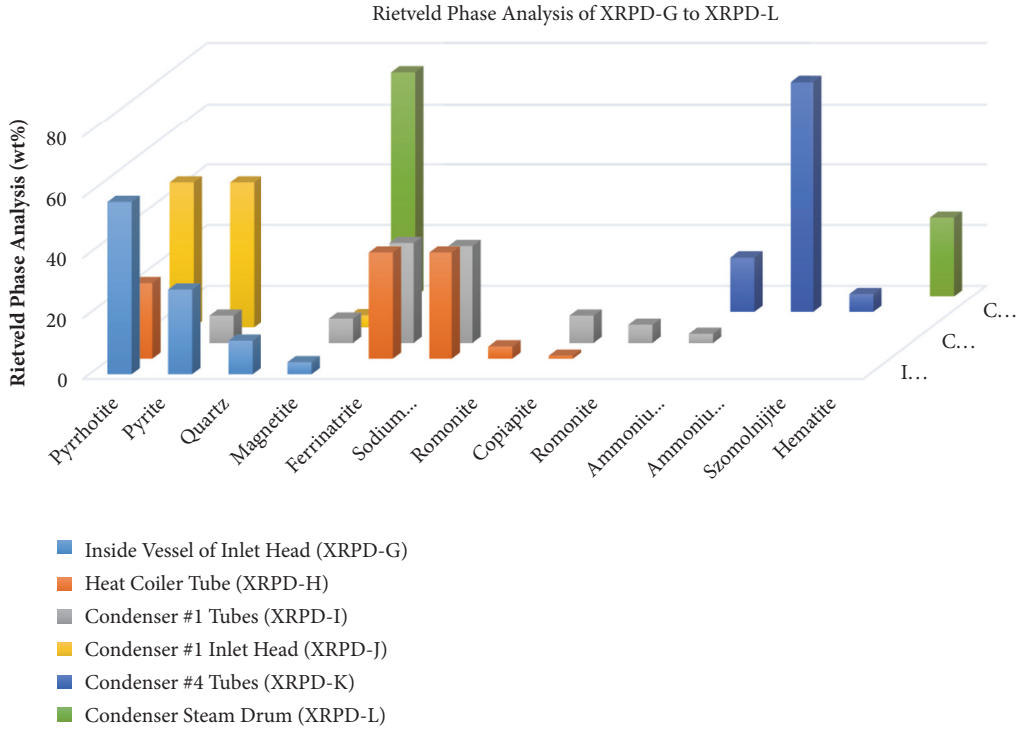

(b) Rietveld phase analysis of XRPD-G to XRPD-L

Figure 5: Rietveld phase analysis results (i.e., wt% of the identified phases) of the inorganic deposit buildup in (a) the condenser tube side #1 (XRPD-D), condenser #4 (XRPD-E), and condenser manway cover (XRPD-F), and (b) the inside vessel of the inlet head (XRPD-G), head coiler tube (XRPD-H), condenser #1 tubes (XRPD-I), condenser #1 inlet head (XRPD-J), condenser #4 tubes (XRPD-K), and condenser steam drum (XRPD-L).

(iii) Equipment of the SRU consisted of iron oxide corrosion products in the steam drum, and iron sulfate corrosion products in the condenser. The presence of dissolved oxygen in the boiler feed water is indicated by a high wt% of iron oxide corrosion product in the form of Fe_3O_4, which appeared in the condenser steam drum.

Knowing which phases quantitatively were involved in the inorganic materials built up in the affected equipment

is a prerequisite required by engineers at the refinery and gas plants to facilitate efficient cleaning of the equipment by drawing up the right procedures and taking preventive action to stop the generation of those particular sludge deposits.

Data Availability

The XRD patterns used to support the findings of this study are available from the corresponding author upon request.

Conflicts of Interest

The authors declare that there are no conflicts of interest regarding the publication of this paper.

Acknowledgments

The authors would like to thank the management of Saudi Aramco for permission to publish this article. Also, the authors would like to thank the help provided by the R&DC/TSD/AAU professionals and technicians.

References

[1] H. Sitepu, R. A. Al-Ghamdi, and S. R. Zaidi, "Application of a New Method in Identifying the Sludge Deposits from Refineries and Gas Plants: A Case of Laboratory-Based Study," *International Journal of Corrosion*, vol. 2017, Article ID 9047545, 7 pages, 2017.

[2] S. N. Smith, "Corrosion Product Analysis in Oil and Gas Pipelines," *Chemical Treatment*, 2004.

[3] H. P. Klug and L. E. Alexander, *X-ray Diffraction Procedures: For Polycrystalline and Amorphous Materials*, John Wiley, New York, NY, USA, 2nd edition, 1974.

[4] F. H. Chung, "Quantitative interpretation of X-ray diffraction patterns of mixtures. III. Simultaneous determination of a set of reference intensities," *Journal of Applied Crystallography*, vol. 8, no. 1, pp. 17–19, 1975.

[5] F. H. Smith and D. K. Smith, *Industrial Applications of X-ray Diffraction*, CRC Press, Taylor & Francis Group, New York, NY, USA, 1st edition, 1999.

[6] W. I. F. David, K. Shankland, L. B. McCusker, and C. Baerlocher, *Structure Determination from Powder Diffraction Data*, Oxford University Press, New York, NY, USA, 2002.

[7] R. E. Dinnebier and S. J. L. Billinge, *Powder Diffraction — Theory and Practice*, Royal Society of Chemistry Publication, 2008.

[8] S. R. Zaidi and H. Sitepu, "Characterization of Corrosion Products in Oil and Gas Facilities Using X-ray Powder Diffraction Method," in *Proceedings of the NACE International Corrosion 2011 Conference and EXPO*, Houston, TX, USA, Papaer 11392, 2011.

[9] S. R. Zaidi, H. Sitepu, and N. M. Al-Yami, "Application of X-ray Powder Diffraction Techniques in Identification of Unknown Materials Formed in Equipment Parts of Sulfur Recovery Unit Plants," *Saudi Aramco Journal of Technology*, 2012.

[10] H. M. Rietveld, "A profile refinement method for nuclear and magnetic structures," *Journal of Applied Crystallography*, vol. 2, pp. 65–71, 1969.

[11] R. A. Young, *The Rietveld Method, International Union of Crystallography*, Oxford University Press, Oxford, UK, 1995.

[12] L. B. Mccusker, R. B. Von Dreele, D. E. Cox, D. Louër, and P. Scardi, "Rietveld refinement guidelines," *Journal of Applied Crystallography*, vol. 32, no. 1, pp. 36–50, 1999.

[13] B. H. Toby and R. B. Von Dreele, "GSAS-II: The genesis of a modern open-source all purpose crystallography software package," *Journal of Applied Crystallography*, vol. 46, no. 2, pp. 544–549, 2013.

[14] B. H. Toby and R. B. Von Dreele, "What's new in GSAS-II," *Powder Diffraction*, vol. 29, no. S2, pp. S2–S6, 2014.

[15] T. Degen, M. Sadki, E. Bron, U. König, and G. Nénert, "The high score suite," *Powder Diffraction*, vol. 29, pp. S13–S18, 2014.

[16] A. Hewat, W. I. David, and L. van Eijck, "Hugo Rietveld (1932–2016)," *Journal of Applied Crystallography*, vol. 49, no. 4, pp. 1394-1395, 2016.

[17] H. Sitepu, R. A. Al-Ghamdi, S. R. Zaidi, and S. Shen, "Use of the Rietveld Method for Describing Structure and Texture in XRD Data of Scale Deposits Formed in Oil and Gas Pipelines: An Important Industrial Challenge," *Advances in X-Ray Analysis*, vol. 58, pp. 41–50, 2015.

[18] H. Sitepu, B. H. O'Connor, and D. Li, "Comparative evaluation of the March and generalized spherical harmonic preferred orientation models using X-ray diffraction data for molybdite and calcite powders," *Journal of Applied Crystallography*, vol. 38, no. 1, pp. 158–167, 2005.

[19] R. J. Hill and C. J. Howard, "Quantitative phase analysis from neutron powder diffraction data using the Rietveld method," *Journal of Applied Crystallography*, vol. 20, no. 6, pp. 467–474, 1987.

[20] B. H. O'Connor and M. D. Raven, "Application of the Rietveld Refinement Procedure in Assaying Powdered Mixtures," *Powder Diffraction*, vol. 3, no. 1, pp. 2–6, 1988.

[21] D. L. Bish and S. A. Howard, "Quantitative phase analysis using the Rietveld method," *Journal of Applied Crystallography*, vol. 21, no. 2, pp. 86–91, 1988.

[22] R. J. Hill, "Expanded use of the rietveld method in studies of phase abundance in multiphase mixtures," *Powder Diffraction*, vol. 6, no. 2, pp. 74–77, 1991.

[23] N. V. Y. Scarlett and I. C. Madsen, "Quantification of phases with partial or no known crystal structures," *Powder Diffraction*, vol. 21, no. 4, pp. 278–284, 2006.

[24] C. Giannini, A. Guagliardi, and R. Millini, "Quantitative phase analysis by combining the Rietveld and the whole-pattern decomposition methods," *Journal of Applied Crystallography*, vol. 35, no. 4, pp. 481–490, 2002.

[25] N. V. Y. Scarlett, I. C. Madsen, L. M. D. Cranswick et al., "Outcomes of the International Union of Crystallography Commission on Powder Diffraction round robin on quantitative phase analysis: Samples 2, 3, 4, synthetic bauxite, natural granodiorite and pharmaceuticals," *Journal of Applied Crystallography*, vol. 35, no. 4, pp. 383–400, 2002.

[26] B. H. O'Connor, D. Y. Li, and H. Sitepu, "Strategies for preferred orientation corrections in X-ray powder diffraction using line intensity ratios," *Advances in X-Ray Analysis*, vol. 34, pp. 409–415, 1991.